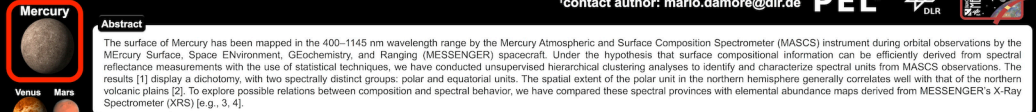


UNSUPERVISED CLASSIFICATION OF MERCURY'S VISIBLE-NEAR-INFRARED REFLECTANCE SPECTRA: COMPARISON WITH MAJOR ELEMENT COMPOSITIONS.

¹Institute for Planetary Research, DLR, Rutherfordstrasse 2, Berlin, Germany; ²Department of Terrestrial Magnetism, Carnegie Institution of Washington, Washington, DC 20015, USA; ³Planetary Science Institute, 1700 E. Fort Lowell, Suite 106, Tucson AZ, 85719, USA; ⁴Physics Department, The Catholic University of America, Washington DC 20064, USA; ⁵Dept. of Earth and Planetary Sciences, American Museum of Natural History, New York, NY 10024, USA; ⁶Lamont-Doherty Earth Observatory, Columbia University, Palisades, NY 10964, USA.

✉contact author: mario.damore@dlr.de   



Abstract

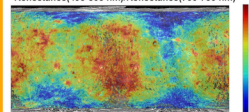
The surface of Mercury has been mapped in the 400–1145 nm wavelength range by the Mercury Atmospheric and Surface Composition Spectrometer (MASCS) instrument during orbital observations by the Mercury Surface, Space Environment, GEochemistry, and Ranging (MESSENGER) spacecraft. Under the hypothesis that surface compositional information can be efficiently derived from spectral reflectance measurements with the use of statistical techniques, we have conducted unsupervised hierarchical clustering analyses to identify and characterize spectral units from MASCS observations. The results [1] display a dichotomy, with two spectrally distinct groups: polar and equatorial units. The spatial extent of the polar unit in the northern hemisphere generally correlates well with that of the northern volcanic plains [2]. To explore possible relations between composition and spectral behavior, we have compared these spectral provinces with elemental abundance maps derived from MESSENGER's X-Ray Spectrometer (XRS) [e.g., 3, 4].

Data Analysis

We use a global hyperspectral data cube image of normalized MASCS visible (VIS) detector spectra to perform our unsupervised hierarchical clustering analysis. Data coverage varies from region to region, but global maps at 1° pixel can be obtained with a high signal-to-noise ratio (SNR). In the absence of a formal global photometric correction for the MASCS data, we have corrected the dataset in an approximate fashion by normalizing all the spectra at 700 nm to account for large variations in observing geometry. We have excluded the most extreme observing geometries by limiting the incidence and emission angles to <85°, which means that latitudes poleward of 80° are excluded. For this analysis we used six spectral channels, each with a bandwidth of 10 nm, in order to focus on “interesting” spectral regions, e.g., bands at ~600 nm that are indicative of sulfides.

MASCS Data Analysis

Reflectance(935-505 nm)/Reflectance(700-750 nm)

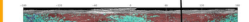


Our approach reveals the existence of two large and spectrally distinct regions, which we call the polar spectral unit (PSU) and the equatorial spectral unit (ESU). Further analysis indicates the presence of smaller sub-units that lie near the boundaries of these large regions and may be transitional areas of intermediate spectral character.

2 Classes Partition



3 Classes Partition

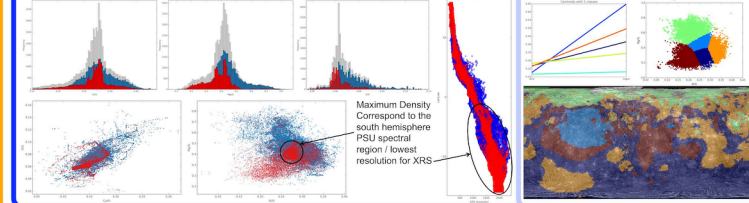


Rembrandt Basin

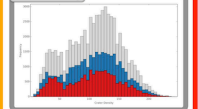
Elemental Maps from XRS

Colors : 2 Classes from MASCS data

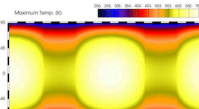
5 Classes from Al/Si and Mg/Si XRS data



Crater Density

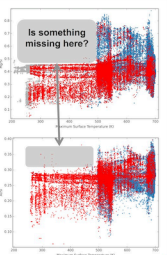


Maximum Temperature

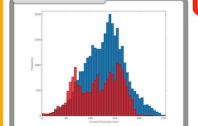


3 Classes from MASCS data

Elemental Ratios vs Max. Temperature



Crustal Thickness



The regional extent of the large-scale spectral units shows good correlation with such datasets as geological unit definition from image mosaics and Gamma-Ray Spectrometer observations [1]. The plains interior to the **Rembrandt impact basin** (PSU and are both examples of relatively young, smooth volcanic deposits. We hypothesize that the spectral characteristics of the PSU originate from material covering an older ESU. Where ESU material is covered by PSU material, fewer hollows (e.g., 5) are observed, which suggests that ESU material is more likely to promote the formation of these landforms [1].

The spectral differences we observe between the PSU and the ESU are also consistent with elemental data derived from the XRS instrument [3, 4]. The **Elemental Maps from XRS** box illustrates several chemical differences between the two spectral clusters. The bimodal frequency distributions for PSU may indicate that the unit is a mixture of two end-member components. The plot of S/Si versus Ca/Si shows an approximately linear relationship for the PSU, whereas the ESU (with a different trend) shows greater departures from a linear relation. This points to a generally more limited distribution of Al/Si in the PSU than in the ESU. It is important to note that the chemical differences are affected by limitations in XRS mapping coverage. XRS data for the PSU originate mainly from the southern hemisphere, where the spatial resolution is poor. Although XRS data for the northern PSU have better spatial resolution, coverage is much more sparse (other than for Mg). Nonetheless, by comparing the VIS/near-infrared MASCS and XRS datasets and investigating the links between them, we can provide further clues to the formation and evolution of Mercury's crust. The **crater density frequency distribution** does not show significant differences between the two spectral classes. This could indicate that the difference marked by these two classes is not directly linked with terrain ages or that this difference could have been erased. The **crustal thickness frequency distribution** does show a bimodal distribution for the PSU, where the two peaks are on the southern hemisphere and on the northern hemisphere with the lower and higher values thickness values respectively. The **simulated maximum surface temperature** show a significant deviation between the two Spectral Units: the PSU distribution peaks around 540 K, where the ESU peaks around much higher temperatures, around 680 K. This implies that the ESU experienced much higher temperatures that could possibly increase sputtering of high volatile elements and drive depletion of those elements in this region. The **maximum surface temperature versus Mg/Si** plot show also an area depleted with points: there is almost no point on the surface with Mg/Si ratio greater ~ 0.48, on region with maximum surface temperature lower of ~ 490 K.

References

[1] Helbert J. et al. (2013) *J. Geophys. Res. Planets*, submitted. [2] Head, J. W. et al. (2011) *Science*, 333, 1853–1856. [3] Nitler L. R. et al. (2011) *Science*, 333, 1847–1850. [4] Weider S. Z. et al. (2012) *J. Geophys. Res.*, 117, E00L06. [5] Bowett D. T. et al. (2011) *Science*, 333, 1856–1859. [6] Nitler L. R. et al. (2013), *LPS XLIX*, Abstract #2458.

Acknowledgment

Thanks to the Scikit-learn community for the Machine Learning tools. “Scik-learn: Machine Learning in Python”, Pedregosa et al., *JMLR* 12, pp. 2825-2830, 2011. <http://scikit-learn.org/>
 Thanks to Christopher Beaumont for his Glue data exploration tool and his personal support. “Multidimensional Data Exploration with Glue”, Beaumont et al., Proceedings of the 12th Python in Science Conference, pp. 8–12, 2013. <http://www.gluviz.org/>
 Thanks to all co-author for their support, to Simone Marchi for the Crater Density data and the whole MESSENGER team.